Validity of One-Dimensional Equation Governing Extrusion Die Flow

Yun-Wey Yu, Ping-Yao Wu and Ta-Jo Liu
Dept. of Chemical Engineering, National Tsing Hua University, Hsinchu, Taiwan 30043, R.O.C.

Recently Weinstein and Ruschak (1996a,b) presented two theoretical studies on fluid flow inside an extrusion die. They examined the 1-D governing equation for flow in the cavity and proposed a new approach to obtain analytical results for shear-thinning fluids (1996a) and also provided a rigorous proof to clarify the differences among previous works on modeling the inertial effect (1996b).

Since 1-D modeling is a simplified approach, they also suggested a systematic procedure which consists of three steps for die design. The first step is to select proper geometry and dimensions of the extrusion die through the effort of 1-D modeling, then complete 3-D simulations will follow to make necessary modifications, and finally, experimental verifications and corrections will be implemented. However, no results regarding the 3-D computation or experimental checkup were presented in their articles.

Experimental verifications of theoretical predictions on extrusion die flows are rarely found in open literature. Lee et al. (1990) and Wen et al. (1994) applied a flow visualization technique to observe the streamlines in cavities and found that the 2-D and 3-D finite-element simulations could predict the flow field satisfactorily. To perform a meaningful experimental verification on the lateral flow uniformity, the extrusion die has to be wide and precisely built; such a die is expensive and it is unlikely that academic researchers would possess it for flow experiments. On the other hand, information regarding the die flow experiment is seldom released by industry. Therefore, the validity of the 1-D modeling on die flow can only be examined in open literature by the 3-D numerical simulation under the present circumstances.

Wu et al. (1995) already verified the accuracy of 1-D modeling and also combined the 1-D model with the 3-D computation for die design. The inertial effect was examined by Wen et al. (1994) with the 3-D finite-element simulation. The power-law model was selected to describe the non-Newtonian viscosity in these two studies.

Weinstein and Ruschak (1996a) and Yuan (1995) argued the shear rates in the cavity or in the slot of an extrusion die can be low enough so that the power-law model is no longer valid and the flow may be Newtonian, therefore, they devised two different approaches to realistically represent the fluid rheology in the cavity and in the slot.

In this note, we shall examine the validity of different 1-D modeling approaches by checking the predictions with the 3-D finite-element simulations. The usefulness of 1-D modeling and important design considerations are also discussed.

Mathematical Formulation

To simplify our discussions, we select a single-cavity linearly tapered extrusion die for illustration. The die geometry is the same as that specified by Lee and Liu (1989) and Yuan (1995). Both Yuan (1995) and Weinstein and Ruschak (1996a) argued that the characteristic shear rate $\dot{\gamma}_c$ in the cavity or in the slot of an extrusion die may be low enough and the power-law model fails to cover such a situation. So, it is appropriate to select the following truncated power-law model (Yuan, 1995)

$$\eta = \zeta \dot{\gamma}^{n-1} \tag{1a}$$

if

$$\dot{\gamma} \geq \dot{\gamma}_c, \quad \zeta = m \tag{1b}$$

if

$$\dot{\gamma} \leq \dot{\gamma}_c, \quad \zeta = \eta_0, n = 1 \tag{1c}$$

m, η_0, and n are the consistency index, zero-shear-rate viscosity, and power-law index, respectively.

The 1-D model consists of the following three equations (Lee and Liu, 1989; Weinstein and Ruschak, 1996b)

(i) 1-D Equation for the Cavity

$$\frac{d\bar{p}}{d\bar{x}}\cos\theta = -\frac{2\rho\beta}{\bar{h}^4}\bar{Q}\frac{d\bar{Q}}{d\bar{x}} + \frac{2\rho\beta}{\bar{h}^5}\bar{Q}^2\frac{d\bar{h}}{d\bar{x}} - \frac{\bar{Q}^{n_c}\zeta}{\kappa^{n_c}\bar{h}^{3+1/n_c}} \tag{2}$$

where $\bar{x}$ is perpendicular to the machine direction. κ and β represent the viscous and the inertial cavity shape factors, respectively, and their precise definitions can be found elsewhere (Lee and Liu, 1989). θ, $\bar{Q}$, $\bar{p}$, and ρ are the die angle, volumetric flow rate, pressure, and density, respectively. $\bar{h}$ is

Correspondence concerning this article should be addressed to T.-J. Lu.

the characteristic length. Here, we take it as the square root of the cross-sectional area of the cavity.

(ii) 1-D Equation for the Slot

$$\bar{q} = \frac{W^{2+1/n_s}}{Am^{1/n_s}}\left(-\frac{d\bar{p}}{d\bar{y}}\right)^{1/n_s} \tag{3}$$

where $\bar{y}$ is the machine direction, $A = 2^{1+(1/n_s)}[2+(1/n_s)]$ and $\bar{q}$ is the volumetric flow rate per unit width. The subscripts c and s denote the power-law index in the cavity and in the slot, respectively.

(iii) Material Balance between the Cavity and the Slot

$$\frac{d\bar{Q}}{d\bar{x}} = -\bar{q} \tag{4}$$

The corresponding boundary conditions are

$$\bar{x} = 0, \quad \bar{Q} = Q_0 \tag{5a}$$

$$\bar{x} = L, \quad \bar{Q} = 0 \tag{5b}$$

and we may define the following dimensionless variables

$$q = \bar{q}/(Q_0/L), \quad p = \bar{p}/p_0, \quad y = \bar{y}/\ell, \quad h = \bar{h}/h_0$$

and

$$p_0 = \ell\left(\frac{Q_0}{\beta_1 L}\right)^{n_s}, \quad \beta_1 = \frac{w^{2+(1/n_s)}}{Am^{1/n_s}}, \quad Re = \frac{\rho\left(\frac{Q_0}{Lw}\right)^{2-n_s} w^{n_s}}{m} \tag{6}$$

where ℓ is the length of the die land. Introducing the dimensionless variables, then Eqs. 2–5 become

(iv) 1-D Cavity Equation

$$\frac{dp}{dx} = Re\left(-N_m Q\frac{dQ}{dx} + N_n\frac{dh}{dx}Q^2\right) - N_\nu Q \tag{7}$$

where

$$N_m = \frac{2\beta w^3 L^2}{\ell h^4 h_0^4 A^{n_s}\cos\theta}, \quad N_n = \frac{2\beta w^3 L^2}{\ell h^5 h_0^5 A^{n_s}\cos\theta}$$

$$N_\nu = \frac{\zeta L^{n_s+1} w^{2n_s+1}}{\kappa^{n_c} Q_0^{n_s-n_c} A^{n_s} m (hh_0)^{3+1/n_c}\cos\theta} \tag{8}$$

(v) 1-D Slot Equation

$$\frac{dQ}{dx} = -\left(\frac{\ell}{\ell - L\tan\theta}p\right)^{1/n_s} \tag{9}$$

(vi) Material Balance

$$\frac{dQ}{dx} = -q \tag{10}$$

and the boundary conditions are

$$x = 0, \quad Q = 1 \tag{11a}$$

$$x = 1, \quad Q = 0 \tag{11b}$$

Since the slot gap is usually very narrow, it is unlikely that the characteristic shear rate in the slot is lower than $\dot{\gamma}_c$ in most practical situations. So we may assume that the shear-thinning behavior is valid in the slot section and only consider the situations that flow in the cavity may be Newtonian or shear-thinning. We shall compare the predictions of the following four 1-D modeling approaches:

(A) *Newtonian cavity flow approach:* this is the approach only for comparison; here the cavity flow is assumed to be Newtonian, irrespective of shear rate.

(B) *Truncated power-law approach of Yuan (1995):* Yuan suggested that one should check the average wall shear rate $\dot{\gamma}_w$ along the cavity against $\dot{\gamma}_c$, if $\dot{\gamma}_w < \dot{\gamma}_c$, n_c is assigned to be unity in Eq. 8.

(C) *Analytical switching approach of Weinstein and Ruschak (1996a):* they took a linearization procedure and derived switching criteria to predict whether the fluid in the cavity is Newtonian or not, an analytical solution was obtained for the flow distribution.

(D) *Standard power-law approach of Lee and Liu (1989):* here the fluid is assumed to obey the power-law model both in the cavity and in the slot, irrespective of shear rate.

Apparently (A) and (D) are two limiting cases.

It is important to note that one of the advantages to apply the 1-D model is that the simple concept of "optimal design" can be easily implemented. Consider the case with the Reynolds number being zero. If we want to design an extrusion die that delivers a liquid sheet with perfect lateral uniformity, we may specify $q = 1$ and from Eq. 10 we have

$$Q = 1 - x \tag{12}$$

If we select the cavity taper function h to be the free geometric parameter that should be arranged to satisfy Eq. 7, by substituting $q = 1$ and Eq. 12 into Eq. 7, we have

$$h = (1-x)^{n_c/(3n_c+1)} \tag{13}$$

and

$$h_0 = \left(\frac{L^{n_s} w^{2n_s+1}\csc\theta}{A^{n_s}\kappa^{n_c}}\right)^{1/(3n_c+1)} \tag{14}$$

The above results were derived by Liu et al. (1988). Note here h is independent of Q_0, η_0, and m.

This "optimal design" method is also applicable to Approach (A), and we have found that h is the same as Eq. 13 but h_0 is as follows ($n_c = 1$)

$$h_0 = \left(\frac{L^{n_s} w^{2n_s+1}\csc\theta\,\eta_0}{Q_0^{n_s-1} A^{n_s}\kappa m}\right)^{1/4} \tag{15}$$

here h_0 is dependent on Q_0, η_0, and m.

As for 3-D computation, we follow the work of Wen et al. (1994); only now we use the Carreau model instead of the power-law model, and η is as follows

$$\eta = \eta_0 (1 + (\lambda \dot{\gamma})^2)^{n - 1/2} \tag{16}$$

Here λ is the characteristic relaxation time.

There are center-fed and end-fed extrusion dies (Wen et al., 1994). The 1-D models do not consider the entrance effects, so we select the end-fed die for comparison because it fits the 1-D models better. The fully developed velocity profile is assumed to exist at the entrance of the cavity. A flat velocity profile is also studied for comparison. Practically speaking, a fully developed velocity profile can be created with a longer inlet duct and a flat velocity profile with a screen (Wen et al., 1994).

Example Calculations

The geometric parameters of the extrusion die are given in Table 1 and the polymeric liquid we select for illustration is a linear polystyrene dissolved in 1-chloronaphthalene (Yasuda et al., 1981), and the rheological data of this fluid fits the Carreau model with $\eta_0 = 166$ Pa·s, $\lambda = 0.0173$ s and $n = 0.538$. The density of the solution is 0.45 g/cm^3. The critical shear rate $\dot{\gamma}_c$ was found to be 57.8 1/s. We may examine the effect of the characteristic shear rate in the cavity by varying the inlet volumetric flow rate Q_0. The Reynolds number for flow in the cavity can be defined as $Re_c = (\rho v_{ave} h_0 / \eta_0)$, where v_{ave} is the average velocity at the inlet plane of the cavity, then for $Q_0 = 100$ cm^3/s, $Re_c = 0.027$, so we can neglect the inertial effect for $Q_0 \leq 100$ cm^3/s.

It should be noted that the Approach (B) predicts that if $Q_0 \geq 15.4$ cm^3/s, part of the cavity flow begins to exhibit shear-thinning behavior. For example, if we select $Q_0 = 50$ cm^3/s, the shear-thinning region exists in the range $0 \leq \bar{x} \leq 60$ cm, and owing to low flow rate, the fluid is Newtonian near the end of the cavity. Approach (C) requires a critical shear rate to be determined, above which the fluid is shear-thinning and this critical shear rate appears at $Q_0 = 11.6$ cm^3/s. We shall present the comparisons by selecting three different inlet flow rates.

Figure 1 displays the results for $Q_0 = 5$ cm^3/s; the cavity flow remains to be Newtonian. Approach (D) deviates from the 3-D simulation as expected, and the other three approaches give relatively accurate predictions. The data for $Q_0 = 12.7$ cm^3/s are shown in Figure 2, since the characteristic shear rate at this flow rate is very close to the critical shear rate that separates the Newtonian and shear-thinning regions; all four approaches generate solutions that are close enough to the 3-D simulation. The results for $Q_0 = 50$ cm^3/s is displayed in Figures 3; it is observed that Approaches

Table 1. Dimensions of the Linearly Tapered Extrusion Die for Illustration

Geometric Parameters	Dimensions
Die width	70 cm
Die angle	0°
Length of die land	1.5 cm
Slot gap	0.025 cm
Cavity shape	semi-60°-tear-dropped
Cross-sectional area of cavity	$(1 - \bar{x}/70)^{0.5}$ cm^2

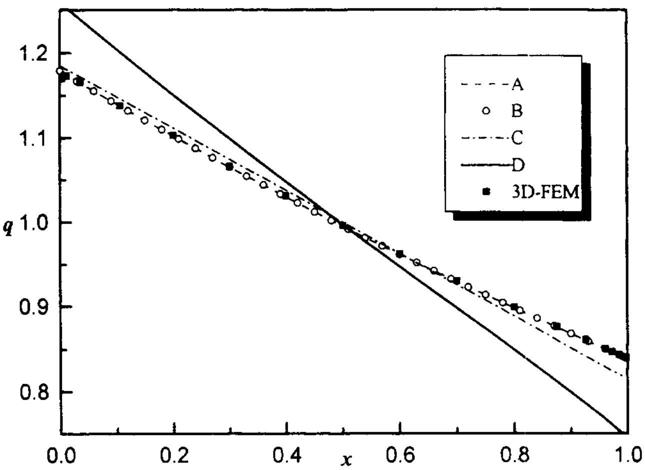

Figure 1. Comparisons of lateral flow distributions between the four 1-D models with 3-D simulation.

$Q_0 = 5$ cm^3/s and Re_c is negligible.

(B)–(D) give accurate predictions, whereas Approach (A) is incorrect under such flow rates as expected.

To examine the inertial effect, we divided the viscosity data of the test solution by a factor 10^3 and repeated the calculations with other variables unchanged. We found that the results for $Q_0 = 5$ cm^3/s and $Q_0 = 12.7$ cm^3/s are almost identical as those without reducing the viscosity. For the case $Q_0 = 50$ cm^3/s and $Re_c = 13.5$, the data in Figure 4 indicate the Approaches (B) and (D) still yield solutions with reasonable accuracy. If Q_0 is increased to 100 cm^3/s and $Re_c = 27$, the results imply that the 1-D modeling is no longer applicable.

Conclusions and Discussions

Even though the example calculations presented here cannot be exhaustive, we still may derive some important conclusions.

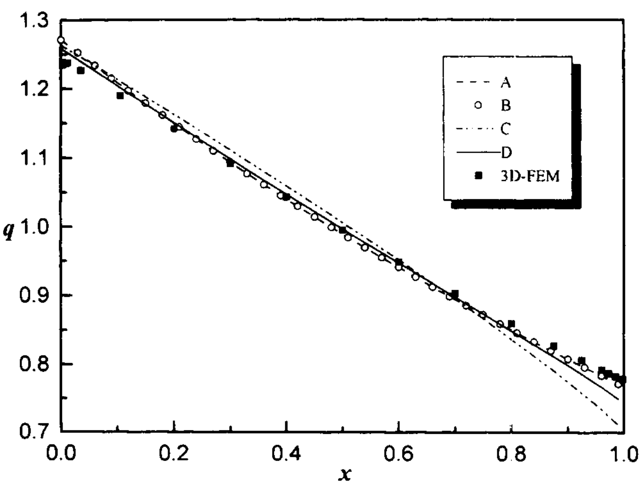

Figure 2. Comparisons of lateral flow distributions between the four 1-D models with 3-D simulation.

$Q_0 = 12.7$ cm^3/s and Re_c is negligible.

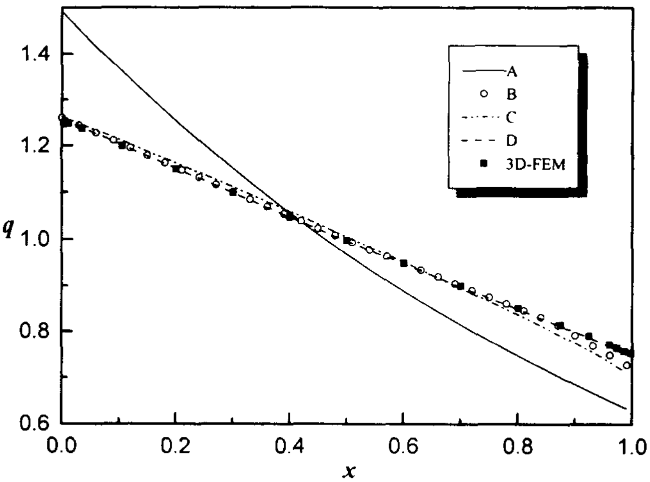

Figure 3. Comparisons of lateral flow distributions between the four 1-D models with 3-D simulation.

$Q_0 = 50$ cm^3/s and Re_c is negligible.

The examples we chose for illustration exhibit "bad" lateral flow distribution as indicated by the figures, and the difference between the maximum and minimum flow rates can be over 20%. The data in Figures 1–3 clearly indicate that the 1-D models can predict the flow distributions with reasonable accuracy. Therefore, one may apply the 1-D modeling with confidence even if the flow distributions have 15–20% difference along the die width.

It is worth noting regarding the 3-D computations that if a flat velocity profile is imposed to replace the fully developed velocity profile at the entrance of the cavity, a small peak of q would appear near $x = 0$, but it has little effect on the flow uniformity. The entrance effects were examined with 3-D computations by Wen et al. (1994), and it appears that these effects are negligible for the example calculation we present here. The 1-D models may not be applicable at the end of the cavity; the results of the 3-D computations indicate that the flow rates at the end of the cavity will rise. However, the flow distribution will be smoothed by the slot section, therefore, the end effect does not appear in the figures.

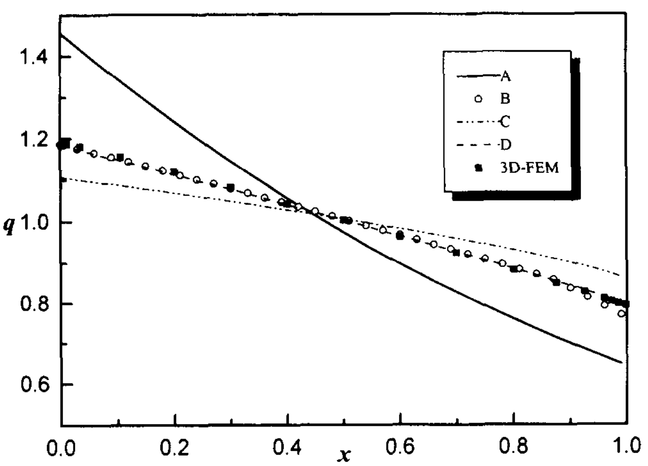

Figure 4. Comparisons of lateral flow distributions between the four 1-D models with 3-D simulation.

$Q_0 = 50$ cm^3/s and $Re_c = 13.5$.

All four models are reasonable accurate provided the characteristic shear rates in the cavity meet the assumption of the models. We have tested several cases with flow nonuniformity less than 10%, and the predictions of Approach (C) are most identical as those of Approaches (A) or (D). However, as the flow nonuniformity rises to 20%, the linearized scheme of Approach (C) can no longer be well matched with Approaches (A) or (D); the differences are observed with the data presented in Figures 1–3. One may conclude that Approaches (B) and (C) can handle both Newtonian and shear-thinning behavior of cavity flow and should be favorable. However, in practical situations, there are certain important considerations that should not be overlooked. For example, one may observe from Eq. 13 and Eq. 14 that the optimal taper function $\bar{h}$ is independent of Q_0, η_0 and m, therefore, if the shear rate can be maintained high enough so that the fluid flow is shear-thinning in the cavity, the flow distribution is independent of the flow rate and the consistency index. This is advantageous, because it allows more freedom for production variations. On the other hand, if the fluid flow is Newtonian in the cavity, $\bar{h}$ will be dependent on Q_0, η_0, and m. Actually for most polymeric liquids, values of the critical shear rate $\dot{\gamma}_c$ fall in the range of $10^{-2} \sim 10^2$ 1/s and it is easy to select the dimensions of the cavity such that the characteristic shear rate in the cavity can be maintained much higher than $\dot{\gamma}_c$ to avoid the solution to be Newtonian. In addition, higher shear rates (or flow rates) in the cavity can reduce the residence time of polymeric liquids in the extrusion dies, shorter residence time is usually helpful to production and quality control. There are only a few exceptions such that applying Approaches (B) or (C) is inevitable because the critical shear rate $\dot{\gamma}_c$ may be as high as $10^3 \sim 10^4$ 1/s (Blake et al., 1995).

The comparisons also show that one has to be careful for handing the inertial effect with the 1-D models; examination by 3-D computation is necessary if the inertial effect is not negligible.

Literature Cited

Blake, T. D., R. Dobson, G. N. Batts, and W. J. Harrison, "Coating Processes," U.S. Patent No. 5,391,401 (1995).

Lee, K. Y., and T. J. Liu, "Design and Analysis of a Dual-Cavity Coat-Hanger Die," *Poly. Eng. Sci.*, **29**, 1066 (1989).

Lee, K. Y., S. H. Wen, and T. J. Liu, "Vortex Formation in a Dual-Cavity Coat-Hanger Die," *Poly. Eng. Sci.*, **30**, 1220 (1990).

Liu, T. J., C. N. Hong, and K. C. Chen, "Computer-Aided Analysis of a Linearly Tapered Coat-Hanger Die," *Poly. Eng. Sci.*, **28**, 1517 (1988).

Weinstein, S. J., and K. J. Ruschak, "Asymptotic Analysis of Die Flow for Shear-Thinning Fluids," *AIChE J.*, **42**, 1501 (1996a).

Weinstein, S. J., and K. J. Ruschak, "One-Dimensional Equations Governing Single-Cavity Die Design," *AIChE J.*, **42**, 2401 (1996b).

Wen, S. H., T. J. Liu, and J. D. Tsou, "Three-Dimensional Finite Element Analysis of Polymeric Fluid Flow in an Extrusion Die: I. Entrance Effect," *Poly. Eng. Sci.*, **34**, 827 (1994).

Wu, P. Y., L. M. Huang, and T. J. Liu, "A Simple Model for Heat Transfer Inside an Extrusion Die," *Poly. Eng. Sci.*, **35**, 1714 (1995).

Yasuda, K., R. C. Armstrong, and R. E. Cohen, "Shear Flow Properties of Concentrated Solutions of Linear and Star Branched Polystyrenes," *Rheol. Acta*, **20**, 163 (1981).

Yuan, S. L., "A Flow Model for Non-Newtonian Liquids Inside a Slot Die," *Poly. Eng. Sci.*, **35**, 577 (1995).

Manuscript received Apr. 22, 1997, and revision received June 17, 1997.